BEAM DYNAMICS OF FUNNELING MULTIPLE BUNCHES ELECTRONS

E. Wang, I. Ben-zvi, D.M. Gassner, W. Meng, T. Rao, E. Riehn, J. Skaritka
Brookhaven National Laboratory, Upton, NY 11973, USA
O. Rahman, Stonybrook, NY 11974,USA

Abstract

The future electron ion collider (eRHIC) at Brookhaven National Laboratory requires a polarized electron source with high average current, short bunch length, and small emittance. The-state-of-the-art single polarized electron photocathode is far from delivering the required 50mA current due to ion back-bombardment limiting the cathode's lifetime and surface charge limit. In our design of the funnelling gun, currently under construction, the electron bunches generated from 20 photocathodes in a 220 kV DC gun are funnelled into a single common beam-axis. This article details design of the optics of our high-average-current polarized electron gun, and presents our simulation of the beam's dynamics and the design of the combiner. We also report herein our progress in constructing the funnelling gun.

INTRODUCTION

A key technological demand in constructing a future heavy-ion collider lies in assuring a high average-current, high-bunch-charge polarized electron source. To meet the requirements for luminosity and electron energy for an electron- and heavy-ion-collider, we are developing a polarized electron source with an average current of 50mA, and a 2.3A peak current. The quantum efficiency (QE) lifetime due to ion back-bombardment limits the level of the achievable average current, and bunch charge with a single GaAs photocathode in a DC gun. One approach to extending charge lifetime is to funnel the electron bunches generated from several photocathodes to a single common axis. In our design, each photocathode generates an average current of 2.5 mA. We placed twenty GaAs photocathodes along the rim of a 32 cm-diameter cathode electrode at a potential of -220 kV. A series of fixed magnetic field dipoles first bend the off-axis electron bunches that then are merged into the main axis by a rotating magnetic field. Figure 1 is the schematic layout of the funnelling gun for transporting current from the cathodes to the depressed collector that acts as a beam dump. Each cathode produces an electron bunch with a 700 kHz of repetition rate. The timing of the radiating laser to the cathode is such that each cathode emits with delay of 70ns after the previous one. After funnelling, the bunches' repetition frequency is 14 MHz; the total average current reaches 50 mA.

*Work supported by Brookhaven Science associates, LLC under Contracts No.DE-AC02-98CH10886 with the U.S.DOE
#wange@bnl.gov

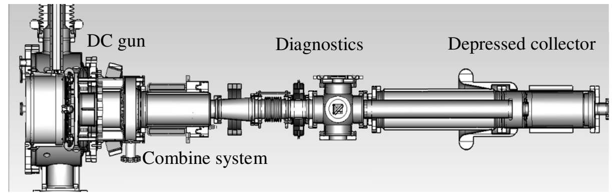

Figure 1: Schematic layout of funnelling gun.

GUN SETUP

The detailed design oft the gun was described earlier [1].We used a Pierce-like DC gun to accelerate the electrons. A focusing field near the cathode balances the effect of the strong space-charge from the bunch. The optimized angle between the cathode and the cathode's electrode is 157°; the gap voltage is 220V across 2.8mm. The maximum field on the cathode is 5.3MV/m. Solenoids placed after the anodes compensate for the defocusing of the space charge in the gun's DC gap. We designed compensated dogleg trajectories in the beam's funnelling system encompassing 20 fixed bending fields, one for each cathode, generated by 20 dipole-magnets, along with a single rotating bending-field generated by the magnetic combiner. Several components of the beam diagnostics are sited downstream, and finally, the beam will absorbed by a depressed collector. Two solenoids downstream of the combiner maintain the beam size.

SIMULATION OF THE COMBINER FIELD

We are using 20 dipole coils and 40 quadrupole ones with a sine AC current to generate rotational dipole- and quadrupole fields [2]. The OPERA AC steady-state solutions confirmed the degree of rotation of the fields, and also that the multicathode emitted beams are in phase. The effect on the beam of the rotating time-dependent field can be ignored. In simulating the gun , we used the static-field maps generated by Opera-3D/TOSCA for simulating the 3D beam in CST Particle Studio. We also generated a rotation dipole- and quadrupole-field from CST EM studio time-domain solver. The 20-sine excition signal is sent to the dipoles; each of them has an 18-degree phase shift. We obtained the animation of the rotating field in the time frame. We used the same setup for generating the rotational quadrupole field. Figure 2 shows the field distribution simulated by CST. The simulated rotated field was used in a PIC solver to assess the the funneling of the multiple bunches . However, the simulation consumed too much time and power due to the RAM limitation in the personal computer and its I/O speed.

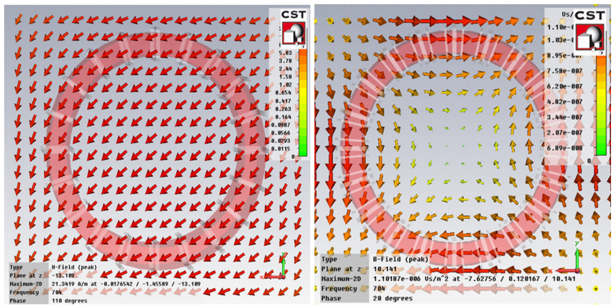

Figure 2: Dipole-field (left) and Quadrupole-field (right) of combiner simulated by CST.

BEAM DYNAMICS

The main problems in beam dynamics are the high bunch-charge, the three-dimensional geometry of the beam's path, and the non-axial symmetricity of the field at the DC gap and at the combiner's entrance about the beam's axis. Therefore, we studied the beam dynamics of the gun and the design of the beam line's optics using "Particle Studio", the 3D beam-tracking code and Particle In Cell (PIC) code developed by Computer Simulation Technology (CST). The following were the three goals of designing the beam line's optics for this gun : i) Prevent the beam from approaching the beam pipe; ii) minimize the beam's emittance at the place of diagnostic cross position, and, iii) focus the beam into the depressed collector. We started by simulating a single beam. The 3D CST Particle studio's tracking solver was used to obtain the beam's transverse parameters. Table I summarizes the optimized input parameters for the simulations.

Table I: Input parameters after optimization

Parameter	Value
Bunch charge	3.5nC
Longitudinal distribution	Gaussian distribution(σ=1.5ns)
Transverse distribution	Uniform
Bunch length at cathode	1.5ns
Bunch radius at cathode	4mm
Thermal emittance, ε_{th}	0.5 μm/mm(rms)
DC gap voltage	220kV
Combiner	Center field=24.5G; Physical length=20cm
First solenoid	Maximum field=560G; Physical length=5.4cm
Second solenoid	Maximum field=184G; Physical length=10.5cm
Third solenoid	Maximum field=366G; Physical length=6.3cm

The current density from the cathode is 4.6A/cm^2, i.e. lower than the limit of GaAs surface charge. Figure 3 shows that the beams' envelope and its transverse normalized RMS emittance as a function of distance with and without the combiner's quadrupole field.

The space-charge force at a 3.5nC bunch with 220keV energy dominates the growth of emittance. The combiner that generates a rotating dipole and a rotating quadrupole magnetic field is synchronized to the beam. Without the quadrupole, the beam lacks focusing in the direction of bending, but experiences excess focusing in the direction of the field. Changing the quadrupole current will equalize the focusing effect in two transverse directions; we obtained a diameter of 15 mm in the round beam's profile at the diagnostic cross when we apply a 7.5A current on the quadrupole coils wherein the divergence angle is x'/y'=23.6mrad/25.1mrad. The transverse normalized RMS emittance is $\varepsilon_{n,x}$/ $\varepsilon_{n,y}$=17.0mm mrad/14.9mm mrad when a quadrupole current is applied.

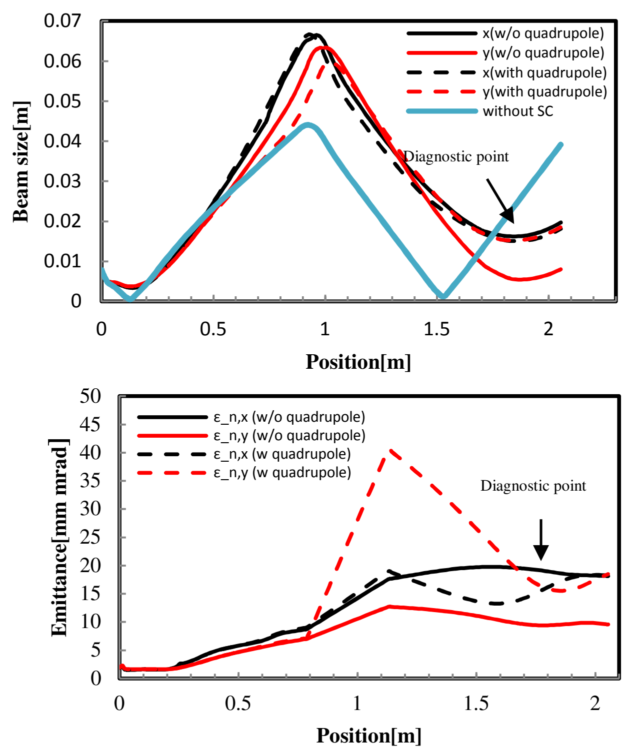

Figure 3 (top): The beam size as a function of distance with and without combiner quadrupole field. The blue curve shows the beam's size without space charge. (bottom) The normalized transverse RMS emittance as a function of distance with and without the combiner's quadrupole field.

Figure 4 illustrates the trajectory of the entire beam line based on the parameters given in Table 1. The beam expands downstream of the diagnostic cross. Therefore, we installed a third solenoid to focus the beam into the depressed collector. The diameter of the beam's waist at the entrance to the collector is 15mm, half that at the collector's entrance aperture. The beam's longitudinal character was simulated using the CST Particle Studio PIC code. The full-beam energy spread at the beam diagnostic cross is 22keV. The energy spread of 97% of the bunch particles is 8keV, viz., an acceptably small energy compared to its energy after the booster.

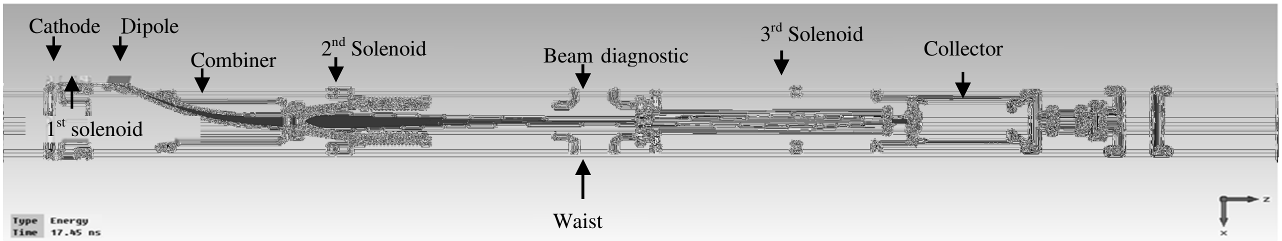

Figure 4: Tracking the entire beam-line. The black curve is the simulated bundle of beam trajectories using the CST particle-tracking solver.

ESTIMATION OF TOLERANCE

A single power-supply will drive the combiner coils' controlling stability to < 25 ppm. The machine's tolerance will be controlled to < 25µm. Based on current's vibration and assembly tolerance on the combiner, we estimate there is 1% non-uniformity transverse distribution on it. The multiple beam size will increase 9.8% and the normalized emittance will increase by 11.3% due to the field tolerance. To get the beam into the entrance aperture of the depressed collector, the tolerance of the timing of the combiner signal allows ±2 degree shift that corresponds to ±8ns.

BEAM-LOSS

Anywhere that a very small fraction of the electron beam strikes the gun's wall, oxidizing gas is desorbed, and the cathode can sustain damage. Several mechanisms contribute to beam loss, such as the formation of a halo round the beam, and the emission of electrons by scattering light or a dark current. We evaluated, in realistic geometry, the loss due to the beam halo by tracking test particles near the beam's edge while modelling the core beam as a slug of charge. The test particles have a different betatron oscillation period from that of the core beam due to defocusing by space charge; this mismatch contributes to the formation of the halo.

We first estimated the position from the cathode at which the beam halo was generated. e. Space-charge changes the force outside the beam, actually reducing the wavelength of betatron oscillation from its value without space charge. We expect the particles at the beam's edge to attain a maximum separation from the beam at one-quarter of that wavelength ($\lambda_+/4$). The following calculation was based on reference [3].The generalized perveance of a single beam-let is 0.0002526 in combiner. For a constant beam radius, we must apply external focusing with the strength k_o^2, where k_o is the betatron wavenumber with no space charge.

$$K_0^2 = \frac{K}{a^2} + \frac{\varepsilon}{a^4}$$

Here, a is the 2*rms beam radius, and ε is the 4*rms non-normalized emittance. K is generalized perveance. We quantify the space-charge force by defining the intensity parameter χ.

$$\chi \equiv \frac{K}{K_0^2 a^2}$$

Using this notation, the reduction in betatron wavelength outside the beam is given by the factor sqrt(1+χ), so the surface particles separate position for the maximum excursion is

$$\frac{\lambda_+}{4} = \frac{2\pi}{4k_0\sqrt{1+\chi}}$$

Based on the beam parameters in Table 1, the calculation results in a distance of 62 cm where the halo beam is generated. It is further downstream of combiner exit.

We also studied the beam's halo by a particle-core model using the PIC code. Two annular-DC electron sources were placed at the cathode and the exit of the first solenoid. The cathode material was set as vacuum to avoid distorting the field. Fifty points uniformly distributed on the imaginary source generated the test particles. We set the average current at 1nA, allowing us to ignore the space-charge force from the test particles. These particles have the same energy and same divergence as the core beam at the site of the imaginary source. Once the beam reaches the annular source, the test particles surrounding the core beam feel its space charge. Tracking their position can identify the mechanism of halo formation and assess beam loss. The bunch approaches the beam pipe at two positions due to lack of focusing upstream of the combiner. One position is at the entrance to the combiner, and another is at the combiner's exit. Our simulation shows that the closest distance between the test particles and aperture at the first position is 11.2mm, and 19.2mm at the second position. Particles at surface of the bunch evidently cannot strike to the beam pipe and desorbs gases. Other mechanisms of beam loss remain to be determined experimentally.

ACKNOWLEDGMENT

The author thanks to Prof. R.A. Kishek for invaluable discussion on beam loss.

REFERENCES

[1] E. Wang, I. Ben-zvi, D. M. Gassner, in *PSTP 2013* (Proceedings of science, Charlottesville, 2013).

[2] I. Ben-Zvi, X. Chang, V. Litvinenko, Physical Review Special Topics - Accelerators and Beams **14**, 092001 (2011).

[3] S. Bernal, B. Quinn, M. Reiser,Physical Review Special Topics - Accelerators and Beams **5**, 064202 (2002).